Hydrothermally enhanced photoluminescence of carbon nanoparticles

Lei Tian,[a,b] Yang Song,[b] Xijun Chang[a,*] and Shaowei Chen[b,*]

[a]Department of Chemistry, Lanzhou University, Lanzhou, Gansu 730000, China
[b]Department of Chemistry and Biochemistry, University of California, 1156 High Street, Santa Cruz, CA 95064, USA

Luminescent carbon nanoparticles were prepared from natural gas soot. The photoluminescence was found to be enhanced more than 10-fold when the particles were subjected to hydrothermal treatment between 200 and 340 °C for up to 15 h. This was accounted for by the effective removal of quinone moieties from the particle surface. Consistent results were obtained from UV–visible, nuclear magnetic resonance, and electrochemical measurements. The correlation may be exploited for controlled manipulation of nanoparticle optoelectronic properties.
© 2010 Acta Materialia Inc. Published by Elsevier Ltd. All rights reserved.

Carbon nanoparticles represent a unique class of carbon-based nanomaterials. Analogous to their well-known cousins, fullerenes and carbon nanotubes, carbon nanoparticles exhibit interesting optical and electronic properties that may be exploited for diverse applications such as optoelectronics, chemical sensing, biological labeling, etc. [1,2]. To this end, various experimental methods have been reported for preparing carbon nanoparticles [3–8], which may exhibit interesting photoluminescence in the visible range. However, so far the molecular origin of nanoparticle photo-emission has remained largely unexplored/unknown. Recently, by adopting a literature procedure [9], we reported a simple and yet effective protocol based on natural gas soot to generate nanosized carbon particles [10]. Experimentally, the soot was collected and underwent refluxing in concentrated nitric acid. Extensive dialysis in nanopure water afforded purified nanoparticles with diameters of around 5 nm, as determined by transmission electron microscopy measurements (Fig. S1, Supplementary data). Structurally, the particles were found to be composed of sp^2 graphitic carbons in the crystalline core with the surface decorated with various oxygenated functional moieties. In addition, the resulting particles exhibited apparent photoluminescence (PL) in the visible range, a phenome-non ascribed to electronic transitions involving surface defect states [10].

In this study, we report the drastic effects of hydrothermal treatments on the PL efficiency of carbon nanoparticles. The enhancement of more than one order of magnitude suggests that trap states on the nanoparticle surface may be effectively reduced by simple hydrothermal treatments. In a typical experiment, 20 mg of carbon nanoparticles were dissolved in 10 ml of nanopure water in a Teflon-lined sealed stainless steel autoclave, which was then placed in a Thermolyne Type F1500 muffle furnace. A programmed temperature profile was adopted to control the heating process. The heating and cooling rates were both set at 1 °C min^{-1}, with the dwell times for certain set temperatures varying from 10 to 900 min. Spectroscopic measurements were then carried out to examine the PL properties of the resulting particles.

Figure 1 depicts the UV–visible absorption spectra of carbon nanoparticles after hydrothermal annealing at 200 °C for various periods of time. It can be seen that before hydrothermal annealing ($t = 0$ min), the particles exhibited a major absorption peak at around 200 nm and another broad peak at ~350 nm. The former was ascribed to the π–π* electronic transitions of internal (sp^2) graphitic carbons, whereas the latter most likely arose from quinone-like functional moieties such as 9,10-phenanthraquinone [11] on the nanoparticle surface, consistent with the voltammetric characteristics observed previously [10]. Interestingly, upon hydrother-

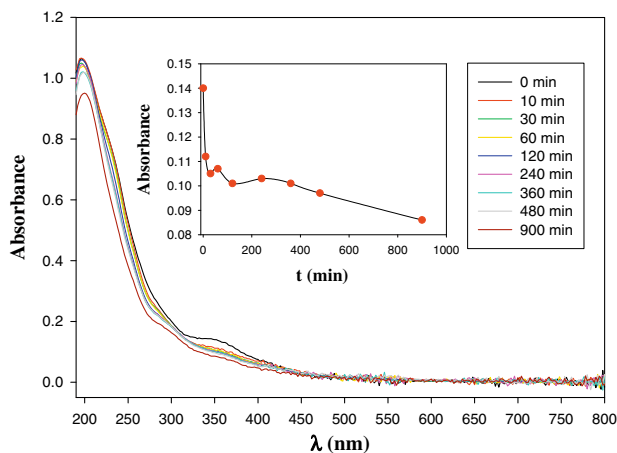* Corresponding authors. Tel.: +831 459 5841; fax: +831 459 2935; e-mail: schen@chemistry.ucsc.edu

Figure 1. UV–visible absorption spectra of carbon nanoparticles after hydrothermal treatments at 200 °C for various periods of time (shown as figure legends). Particle concentrations were all 17.8 μg ml^{-1} in water. Inset shows the variation in the absorbance at 350 nm with heating time.

mal annealing at 200 °C, the peak at 200 nm remained very well-defined, whereas the peak at 350 nm diminished with increasing heating time, as reflected in the inset of Figure 1. In fact, the peak reduction was most apparent in the first 10 min of hydrothermal treatment and continued slowly up to 900 min, suggesting effective removal of the quinone moieties from the nanoparticle surface (see below).

Notably, the resulting particles exhibited drastically enhanced photoluminescence, as compared to those without hydrothermal treatments. Figure 2 shows the excitation and emission spectra of the corresponding carbon nanoparticles before and after hydrothermal treatments in pure water at 200 °C. It can be seen that the excitation and emission peak energies remained practically unchanged at λ_{ex} = 314 nm and λ_{em} = 430 nm, respectively, after hydrothermal treatment, suggesting a similar radiative decay pathway for the photoexcited electrons in the original and heated particles. In sharp contrast, the PL
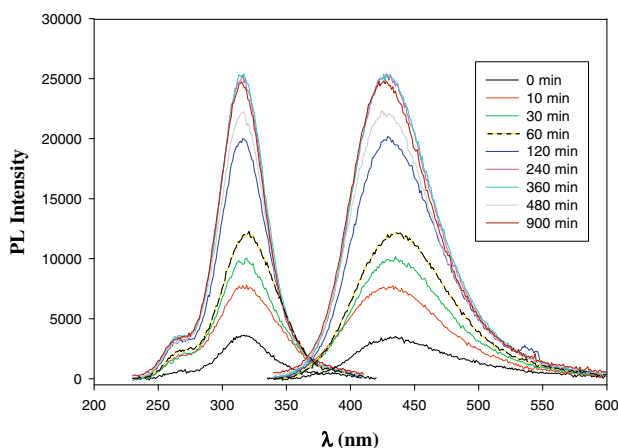

Figure 2. Excitation (left) and emission (right) spectra of carbon nanoparticles before and after hydrothermal treatment at 200 °C for various periods of time (shown as figure legends). Excitation wavelength 314 nm; emission wavelength 430 nm. Particle concentrations were all 17.8 μg ml^{-1} in water.

intensity exhibited drastic enhancement of more than one order of magnitude for the heated samples as compared to the original ones (note that the optical density at the excitation wavelength for these particles was very similar, as depicted in Figure 1), in particular in the first 2 h. At longer heating times (up to 15 h), the intensity appeared to reach a plateau. The corresponding emission quantum efficiency was estimated by using rhodamine 6G as the calibrating reference [10]. The results are summarized in Table 1. It can be seen that for the original particles, the quantum yield was only 0.43%, whereas it increased sharply to 1.63% after 10 min of hydrothermal treatment, and after 900 min, the quantum efficiency increased more than 10-fold to 4.96%. This significant improvement in the emission efficiency is most likely due to the reduction of nonradiative pathways by hydrothermal treatment.

It should be noted that the carbon nanoparticle surface was decorated with a variety of oxygenated functional moieties including quinone derivatives [10], and quinone derivatives are well-known effective electron acceptors [12,13]. Therefore the presence of quinone moieties on the nanoparticle surface might provide a nonradiative pathway for the decay of photoexcited electrons [14,15], thus decreasing the efficiency of particle photoluminescence. From Figure 1, it can be seen that the concentration of quinone derivatives on the particle surface was effectively reduced by hydrothermal treatment, an observation consistent with the drastic enhancement of photoluminescence shown in Figure 2 and Table 1. Additionally, it can be seen that the emission peaks also became narrower after hydrothermal treatment of the nanoparticles, suggesting that defects were indeed annealed, especially those contributing to red emission [16].

The above interpretation was further supported by results from ^{13}C nuclear magnetic resonance (NMR) measurements (Fig. S2, Supplementary data). It can be seen that the overall profiles were similar to that of the original carbon nanoparticles [10]. First, no feature was observed below 120 ppm for all hydrothermally treated samples, indicating the absence of aliphatic (sp^3) carbons within the particles. Second, within the range of 120–180 ppm, a series of peaks emerged. The broad peak centered at 138 ppm was ascribed to internal C=C sp^2 carbons; the peaks between 120 and 130 ppm most likely arose from (polycyclic) aromatic carbons, analogous to those of chrysene, pyrene, etc.; and the peak between 170 and 180 ppm most probably arose from carboxylic/carbonyl C=O carbons. If quinone derivatives were indeed removed by the hydrothermal treatments, one would anticipate a decrease in the C=O peak relative to the C=C one. In fact, the ratio of the integrated areas of the C=O and C=C peaks was estimated to be 2.00 for the original carbon particles. After hydrothermal treatment at 200 °C, this ratio decreased to 1.84 (1 h), and further to 1.14 (6 h); and then increased slightly to 1.21 (15 h). These results indicate that the concentration of carbonyl/carboxylic carbons decreased sharply in the first 6 h and then only moderately at longer heating times.

Consistent behaviors were observed in electrochemical measurements. Figure S3 (Supplementary data) depicts two representative differential pulse voltammo-

Table 1. Photoluminescence quantum yield of carbon nanoparticles after hydrothermal treatment at 200 °C for various periods of time.

Time (min)	0	10	30	60	120	240	360	480	900
Quantum yield (%)	0.43	1.63	2.07	2.58	3.81	4.33	4.12	4.08	4.96

grams (DPVs) of the nanoparticles before and after hydrothermal treatment at 200 °C for 6 h. It can be seen that the as-prepared samples exhibited a pair of rather well-defined voltammetric peaks at $\sim +0.12$ V along with a weak shoulder at ~ -0.02 V. These voltammetric features have been observed previously and ascribed to the redox chemistry of nanoparticle surface functional moieties that were analogous to phenanthrenequinone derivatives [10]. In sharp contrast, after hydrothermal treatment, these voltammetric peaks diminished drastically, suggesting effective removal of the quinone-like moieties from the nanoparticle surface, which is consistent with the ^{13}C NMR measurements presented above.

Further studies were carried out with the heating temperature varied from 160 to 340 °C. It was found that higher temperatures led to more effective removal of the quinone moieties, as manifested by the monotonic diminishment of the absorption peak at 350 nm with increasing hydrothermal temperature (Fig. S4, Supplementary data) as well as in ^{13}C NMR measurements (Fig. S2). For instance, the ratio of the integrated areas of the C=O and C=C peaks was only 0.39 when the hydrothermal temperature was increased to 260 °C.

The decreasing concentration of quinone-like nonradiative traps on the nanoparticle surface was also manifested in the corresponding photoluminescence measurements. Figure 3 depicts the excitation and emission spectra of the carbon nanoparticles after hydrothermal treatments at varied temperatures. It can be seen that the excitation and emission peak energies (λ_{ex}, λ_{em}) remained virtually unchanged at 314 and 450 nm, respectively, at hydrothermal temperatures $\leqslant 200$ °C. However, at higher temperatures, a small but apparent blue-shift emerged: (311 nm, 419 nm) at 260 °C, (309 nm, 406 nm) at 300 °C, and (309 nm, 402 nm) at 340 °C. Interestingly, as the shift in the emission peak energy was far more pronounced than that of the excitation peak

energy, the energy difference between the emission and excitation peaks became smaller. That is, the overall PL profiles were increasingly analogous to band-edge emission with increasing hydrothermal temperature. One would therefore anticipate more efficient PL emission. In fact, the quantum yield for photoluminescence exhibited a rather drastic increase (more than one order of magnitude) at hydrothermal temperatures higher than 200 °C, as compared to that of the original nanoparticles (0.43%, Table 1): 1.26% at 160 °C, 4.12% at 200 °C, 6.24% at 260 °C, 6.05% at 300 °C, and 5.76% at 340 °C, respectively.

Taken together, these studies demonstrate that the PL of carbon nanoparticles might be drastically enhanced by simple hydrothermal annealing at moderately elevated temperatures, by virtue of the effective removal of nonradiative electron acceptors such as quinone moieties from the nanoparticle surface. It is likely that the fundamental mechanism involved in the hydrothermal reactions is analogous to those observed with polycyclic aromatic compounds as well as carbon nanotubes, such as decarboxylation and ring opening [17,18]. Further and more detailed identification of the nanoparticle surface chemistry may be achieved by selective chemical labeling. Research in this direction is currently underway.

Supplementary data include TEM micrographs, differential pulse voltammograms, ^{13}C NMR spectra of carbon nanoparticles after hydrothermal treatments at 200 °C for varied periods of time, and UV–visible spectra of carbon nanoparticles after hydrothermal treatments for 6 h at varied temperatures. Supplementary data associated with this article can be found, in the online version, at doi:10.1016/j.scriptamat.2010.02.035.
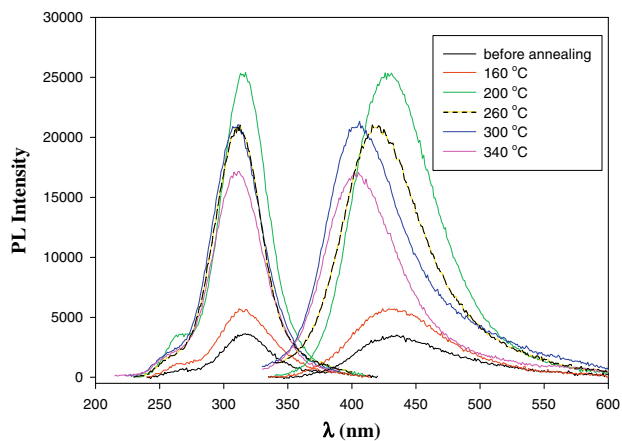

Figure 3. Excitation (left) and emission (right) spectra of carbon nanoparticles before and after hydrothermal treatment for 6 h at various temperatures (shown as figure legends). Particle concentrations were all 17.8 μg ml^{-1} in water.

[1] M.S. Dresselhaus, G. Dresselhaus, Nanostruct. Mater. 9 (1997) 33–42.

[2] M.S. Dresselhaus, Annu. Rev. Mater. Sci. 27 (1997) 1–34.

[3] A.B. Bourlinos, A. Stassinopoulos, D. Anglos, R. Zboril, V. Georgakilas, E.P. Giannelis, Chem. Mater. 20 (2008) 4539–4541.

[4] Q.L. Zhao, Z.L. Zhang, B.H. Huang, J. Peng, M. Zhang, D.W. Pang, Chem. Commun. (2008) 5116–5118.

[5] B.R. Selvi, D. Jagadeesan, B.S. Suma, G. Nagashankar, M. Arif, K. Balasubramanyam, M. Eswaramoorthy, T.K. Kundu, Nano Lett. 8 (2008) 3182–3188.

[6] J. Kua, W.A. Goddard, J. Am. Chem. Soc. 121 (1999) 10928–10941.

[7] Y.P. Sun, B. Zhou, Y. Lin, W. Wang, K.A.S. Fernando, P. Pathak, M.J. Meziani, B.A. Harruff, X. Wang, H.F.

Wang, P.J.G. Luo, H. Yang, M.E. Kose, B.L. Chen, L.M. Veca, S.Y. Xie, J. Am. Chem. Soc. 128 (2006) 7756–7757.

[8] J.G. Zhou, C. Booker, R.Y. Li, X.T. Zhou, T.K. Sham, X.L. Sun, Z.F. Ding, J. Am. Chem. Soc. 129 (2007) 744–745.

[9] H.P. Liu, T. Ye, C.D. Mao, Angew. Chem. Int. Ed. 46 (2007) 6473–6475.

[10] L. Tian, D. Ghosh, W. Chen, S. Pradhan, X.J. Chang, S.W. Chen, Chem. Mater. 21 (2009) 2803–2809.

[11] J.E. Gautrot, P. Hodge, M. Helliwell, J. Raftery, D. Cupertino, J. Mater. Chem. 19 (2009) 4148–4156.

[12] D.K. Newman, R. Kolter, Nature 405 (2000) 94–97.

[13] G. Jones, X.H. Qian, J. Phys. Chem. A 102 (1998) 2555–2560.

[14] J.W. Lee, W. Zipfel, T.G. Owens, J. Luminesc. 51 (1992) 79–89.

[15] S. Rajagopal, E.A. Egorova, N.G. Bukhov, R. Carpentier, Biochim. Biophys. Acta Bioenerg. 1606 (2003) 147–152.

[16] V. Borjanovic, W.G. Lawrence, S. Hens, M. Jaksic, I. Zamboni, C. Edson, I. Vlasov, O. Shenderova, G.E. McGuire, Nanotechnology 19 (2008) 455701-1–455701-10.

[17] G.S. Duesberg, S. Roth, P. Downes, A. Minett, R. Graupner, L. Ley, N. Nicoloso, Chem. Mater. 15 (2003) 3314–3319.

[18] J.A. Onwudili, P.T. Williams, J. Supercrit. Fluids 39 (2007) 399–408.